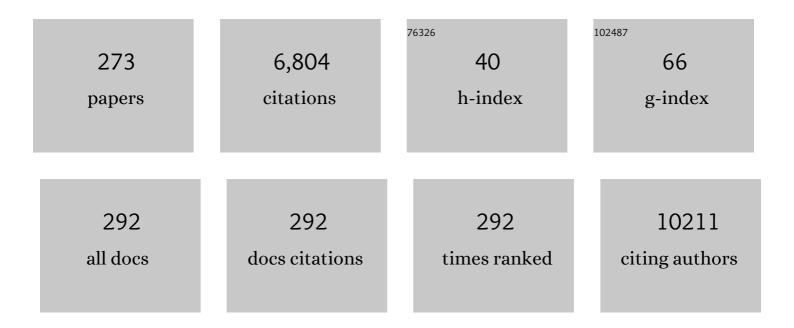
Gi Jeong Cheon

List of Publications by Year in descending order

Source: https://exaly.com/author-pdf/3046786/publications.pdf Version: 2024-02-01



#	Article	IF	CITATIONS
1	Prognostic Value of Metabolic Tumor Volume and Total Lesion Glycolysis in Head and Neck Cancer: A Systematic Review and Meta-Analysis. Journal of Nuclear Medicine, 2014, 55, 884-890.	5.0	257
2	A Hybrid Nanoparticle Probe for Dualâ€Modality Positron Emission Tomography and Magnetic Resonance Imaging. Angewandte Chemie - International Edition, 2008, 47, 6259-6262.	13.8	203
3	Prognostic value of volumetric parameters of 18F-FDG PET in non-small-cell lung cancer: a meta-analysis. European Journal of Nuclear Medicine and Molecular Imaging, 2015, 42, 241-251.	6.4	203
4	Preparation of a Promising Angiogenesis PET Imaging Agent: 68Ga-Labeled c(RGDyK)–Isothiocyanatobenzyl-1,4,7-Triazacyclononane-1,4,7-Triacetic Acid and Feasibility Studies in Mice. Journal of Nuclear Medicine, 2008, 49, 830-836.	5.0	190
5	Tumor-Associated Macrophages Enhance Tumor Hypoxia and Aerobic Glycolysis. Cancer Research, 2019, 79, 795-806.	0.9	188
6	Systemic and Specific Delivery of Small Interfering RNAs to the Liver Mediated by Apolipoprotein A-I. Molecular Therapy, 2007, 15, 1145-1152.	8.2	159
7	11C-Pittsburgh B PET Imaging in CardiacÂAmyloidosis. JACC: Cardiovascular Imaging, 2015, 8, 50-59.	5.3	135
8	Crossâ€calibration of multiâ€frequency bioelectrical impedance analysis with eightâ€point tactile electrodes and dualâ€energy Xâ€ray absorptiometry for assessment of body composition in healthy children aged 6–18â€fyears. Pediatrics International, 2009, 51, 263-268.	0.5	119
9	Intracranial ganglioglioma: preoperative characteristics and oncologic outcome after surgery. Journal of Neuro-Oncology, 2002, 59, 173-183.	2.9	111
10	Prediction Model of Chemotherapy Response in Osteosarcoma by ¹⁸ F-FDG PET and MRI. Journal of Nuclear Medicine, 2009, 50, 1435-1440.	5.0	111
11	Apoptosis-inducing antitumor efficacy of hexokinase II inhibitor in hepatocellular carcinoma. Molecular Cancer Therapeutics, 2007, 6, 2554-2562.	4.1	100
12	Prediction of microvascular invasion of hepatocellular carcinoma using gadoxetic acid-enhanced MR and 18F-FDG PET/CT. Abdominal Imaging, 2015, 40, 843-851.	2.0	98
13	Neuroendocrine differentiation of prostate cancer leads to PSMA suppression. Endocrine-Related Cancer, 2019, 26, 131-146.	3.1	98
14	Recent Trends in PET Image Interpretations Using Volumetric and Texture-based Quantification Methods in Nuclear Oncology. Nuclear Medicine and Molecular Imaging, 2014, 48, 1-15.	1.0	86
15	2016 Revised Korean Thyroid Association Management Guidelines for Patients with Thyroid Nodules and Thyroid Cancer. International Journal of Thyroidology, 2016, 9, 59.	0.1	80
16	Diagnostic Performance of Resting and Hyperemic Invasive Physiological Indices to Define Myocardial Ischemia. JACC: Cardiovascular Interventions, 2017, 10, 751-760.	2.9	80
17	Comparison of 18F-FDG, 18F-FET and 18F-FLT for differentiation between tumor and inflammation in rats. Nuclear Medicine and Biology, 2009, 36, 681-686.	0.6	78
18	Radiomics in Oncological PET/CT: a Methodological Overview. Nuclear Medicine and Molecular Imaging, 2019, 53, 14-29.	1.0	77

#	Article	IF	CITATIONS
19	In Vivo Differentiation of Human Amniotic Epithelial Cells into Cardiomyocyte-Like Cells and Cell Transplantation Effect on Myocardial Infarction in Rats: Comparison with Cord Blood and Adipose Tissue-Derived Mesenchymal Stem Cells. Cell Transplantation, 2012, 21, 1687-1696.	2.5	75
20	Comparison of 4D CT, Ultrasonography, and ^{99m} Tc Sestamibi SPECT/CT in Localizing Singleâ€Gland Primary Hyperparathyroidism. Otolaryngology - Head and Neck Surgery, 2015, 152, 438-443.	1.9	72
21	Integrated Myocardial Perfusion Imaging Diagnostics Improve Detection of Functionally Significant Coronary Artery Stenosis by ¹³ N-ammonia Positron Emission Tomography. Circulation: Cardiovascular Imaging, 2016, 9, .	2.6	67
22	18F-FDG uptake and EGFR mutations in patients with non-small cell lung cancer: A single-institution retrospective analysis. Lung Cancer, 2010, 67, 76-80.	2.0	66
23	Characterization and Cancer Cell Specific Binding Properties of Anti-EGFR Antibody Conjugated Quantum Dots. Bioconjugate Chemistry, 2010, 21, 940-946.	3.6	65
24	Autoclustering of Non-small Cell Lung Carcinoma Subtypes on 18F-FDG PET Using Texture Analysis: A Preliminary Result. Nuclear Medicine and Molecular Imaging, 2014, 48, 278-286.	1.0	60
25	Update on nodal staging in non-small cell lung cancer with integrated positron emission tomography/computed tomography: a meta-analysis. Annals of Nuclear Medicine, 2015, 29, 409-419.	2.2	60
26	Preoperative staging of non-small cell lung cancer: prospective comparison of PET/MR and PET/CT. European Radiology, 2016, 26, 3850-3857.	4.5	58
27	Associations of urinary concentrations of phthalate metabolites, bisphenol A, and parabens with obesity and diabetes mellitus in a Korean adult population: Korean National Environmental Health Survey (KoNEHS) 2015–2017. Environment International, 2021, 146, 106227.	10.0	55
28	Overexpression of Glut1 in lymphoid follicles correlates with false-positive (18)F-FDG PET results in lung cancer staging. Journal of Nuclear Medicine, 2004, 45, 999-1003.	5.0	55
29	PET/CT-Based Dosimetry in 90Y-Microsphere Selective Internal Radiation Therapy. Medicine (United) Tj ETQq1 1	0.784314 1.0	rgBT /Overloo
30	Revival of TE2A; a better chelate for Cu(II) ions than TETA?. Chemical Communications, 2010, 46, 3517.	4.1	53
31	Prognostic Implications of the SUVmax of Primary Tumors and Metastatic Lymph Node Measured by 18F-FDG PET in Patients With Uterine Cervical Cancer. Clinical Nuclear Medicine, 2016, 41, 34-40.	1.3	52
32	Differential Expression of Glucose Transporters and Hexokinases in Prostate Cancer with a Neuroendocrine Gene Signature: A Mechanistic Perspective for ¹⁸ F-FDG Imaging of PSMA-Suppressed Tumors. Journal of Nuclear Medicine, 2020, 61, 904-910.	5.0	52
33	Bone Mineral Density According to Age, Bone Age, and Pubertal Stages in Korean Children and Adolescents. Journal of Clinical Densitometry, 2010, 13, 68-76.	1.2	51
34	Prognostic value of preoperative intratumoral FDG uptake heterogeneity in early stage uterine cervical cancer. Journal of Gynecologic Oncology, 2016, 27, e15.	2.2	50
35	Prognostic value of metabolic tumour volume on baseline 18F-FDG PET/CT in addition to NCCN-IPI in patients with diffuse large B-cell lymphoma: further stratification of the group with a high-risk NCCN-IPI. European Journal of Nuclear Medicine and Molecular Imaging, 2019, 46, 1417-1427.	6.4	49
36	Combined Treatment with Silibinin and Epidermal Growth Factor Receptor Tyrosine Kinase Inhibitors Overcomes Drug Resistance Caused by T790M Mutation. Molecular Cancer Therapeutics, 2010, 9, 3233-3243.	4.1	47

#	Article	IF	CITATIONS
37	Comparison of SPECT/CT and MRI in Diagnosing Symptomatic Lesions in Ankle and Foot Pain Patients: Diagnostic Performance and Relation to Lesion Type. PLoS ONE, 2015, 10, e0117583.	2.5	46
38	A simple Cu-64 production and its application of Cu-64 ATSM. Applied Radiation and Isotopes, 2009, 67, 1190-1194.	1.5	45
39	Influence of Androgen Deprivation Therapy on the Uptake of PSMA-Targeted Agents: Emerging Opportunities and Challenges. Nuclear Medicine and Molecular Imaging, 2017, 51, 202-211.	1.0	45
40	Prognostic value of preoperative intratumoral FDG uptake heterogeneity in patients with epithelial ovarian cancer. European Radiology, 2017, 27, 16-23.	4.5	44
41	Integrated 18F-FDG PET/MRI in breast cancer: early prediction of response to neoadjuvant chemotherapy. European Journal of Nuclear Medicine and Molecular Imaging, 2018, 45, 328-339.	6.4	43
42	18F-Fluoro-2-Deoxy-Glucose Uptake Predicts Clinical Outcome in Patients with Gefitinib-Treated Non–Small Cell Lung Cancer. Clinical Cancer Research, 2008, 14, 2036-2041.	7.0	41
43	Evaluation of lymphedema in upper extremities by MR lymphangiography: Comparison with lymphoscintigraphy. Magnetic Resonance Imaging, 2018, 49, 63-70.	1.8	41
44	High prevalence of osteoporosis in patients with gastric adenocarcinoma following gastrectomy. World Journal of Gastroenterology, 2007, 13, 6492.	3.3	41
45	Radiation sensitivity depends on OGG1 activity status in human leukemia cell lines. Free Radical Biology and Medicine, 2002, 32, 212-220.	2.9	40
46	Implication of Lymph Node Metastasis Detected on 18F-FDG PET/CT for Surgical Planning in Patients With Peripheral Intrahepatic Cholangiocarcinoma. Clinical Nuclear Medicine, 2014, 39, 1-7.	1.3	40
47	[11C]-(R)-PK11195 positron emission tomography in patients with complex regional pain syndrome. Medicine (United States), 2017, 96, e5735.	1.0	40
48	A potential role for skeletal muscle caveolin-1 as an insulin sensitivity modulator in ageing-dependent non-obese type 2 diabetes: studies in a new mouse model. Diabetologia, 2008, 51, 1025-1034.	6.3	39
49	Exploring Coronary Circulatory Response to Stenosis and Its Association With Invasive Physiologic Indexes Using Absolute Myocardial Blood Flow and Coronary Pressure. Circulation, 2017, 136, 1798-1808.	1.6	39
50	Anesthesia condition for 18F-FDG imaging of lung metastasis tumors using small animal PET. Nuclear Medicine and Biology, 2008, 35, 143-150.	0.6	38
51	Diagnostic values of thyroglobulin measurement in fine-needle aspiration of lymph nodes in patients with thyroid cancer. Endocrine, 2015, 49, 70-77.	2.3	38
52	Noninvasive Imaging of Myocardial Inflammation in Myocarditis using ⁶⁸ Ga-tagged Mannosylated Human Serum Albumin Positron Emission Tomography. Theranostics, 2017, 7, 413-424.	10.0	38
53	Prognostic value of preoperative metabolic tumor volume measured by 18F-FDG PET/CT and MRI in patients with endometrial cancer. Gynecologic Oncology, 2013, 130, 446-451.	1.4	37
54	Radioiodine Therapy in Differentiated Thyroid Cancer: The First Targeted Therapy in Oncology. Endocrinology and Metabolism, 2014, 29, 233.	3.0	37

#	Article	IF	CITATIONS
55	Radiation Dose from Whole-Body F-18 Fluorodeoxyglucose Positron Emission Tomography/Computed Tomography: Nationwide Survey in Korea. Journal of Korean Medical Science, 2016, 31, S69.	2.5	37
56	Prediction of Posttransplantation Recurrence of Hepatocellular Carcinoma Using Metabolic and Volumetric Indices of ¹⁸ F-FDG PET/CT. Journal of Nuclear Medicine, 2016, 57, 1045-1051.	5.0	37
57	Synthesis and evaluation of stilbene derivatives as a potential imaging agent of amyloid plaques. Bioorganic and Medicinal Chemistry, 2010, 18, 7724-7730.	3.0	35
58	Usefulness of Integrated PET/MRI in Head and Neck Cancer: A Preliminary Study. Nuclear Medicine and Molecular Imaging, 2014, 48, 98-105.	1.0	34
59	Prognostic Value of Metabolic Tumor Volume on 11C-Methionine PET in Predicting Progression-Free Survival in High-Grade Glioma. Nuclear Medicine and Molecular Imaging, 2015, 49, 291-297.	1.0	34
60	Association of exposure to polycyclic aromatic hydrocarbons and heavy metals with thyroid hormones in general adult population and potential mechanisms. Science of the Total Environment, 2021, 762, 144227.	8.0	34
61	Hepatic siRNA delivery using recombinant human apolipoprotein A-I in mice. Biochemical and Biophysical Research Communications, 2009, 378, 192-196.	2.1	33
62	Positron Emission Tomography/Magnetic Resonance Imaging Evaluation of Lung Cancer. Journal of Thoracic Imaging, 2014, 29, 4-16.	1.5	33
63	188Re-tin-colloid as a new therapeutic agent for rheumatoid arthritis. Nuclear Medicine Communications, 2003, 24, 689-696.	1.1	32
64	Usefulness of MRI-assisted metabolic volumetric parameters provided by simultaneous 18F-fluorocholine PET/MRI for primary prostate cancer characterization. European Journal of Nuclear Medicine and Molecular Imaging, 2015, 42, 1247-1256.	6.4	32
65	18F-FDG PET/CT in Anti-LGI1 Encephalitis. Clinical Nuclear Medicine, 2015, 40, 156-158.	1.3	32
66	Prognostic Value of Metabolic and Volumetric Parameters of Preoperative FDG-PET/CT in Patients With Resectable Pancreatic Cancer. Medicine (United States), 2016, 95, e3686.	1.0	32
67	Exposure to polycyclic aromatic hydrocarbons and volatile organic compounds is associated with a risk of obesity and diabetes mellitus among Korean adults: Korean National Environmental Health Survey (KoNEHS) 2015–2017. International Journal of Hygiene and Environmental Health, 2022, 240, 113886.	4.3	32
68	Real-time Tumor Oxygenation Changes AfterÂSingle High-dose Radiation Therapy inÂOrthotopic and Subcutaneous Lung Cancer inÂMice: Clinical Implication for StereotacticÂAblative Radiation Therapy ScheduleÂOptimization. International Journal of Radiation Oncology Biology Physics, 2016, 95, 1022-1031.	0.8	31
69	Multidisciplinary perspectives on newly revised 2018 FIGO staging of cancer of the cervix uteri. Journal of Gynecologic Oncology, 2019, 30, e40.	2.2	31
70	Clinical impact of whole-body FDG-PET for evaluation of response and therapeutic decision-making of primary lymphoma of bone. Annals of Oncology, 2005, 16, 1401-1402.	1.2	30
71	Heterogeneity index evaluated by slope of linear regression on 18F-FDG PET/CT as a prognostic marker for predicting tumor recurrence in pancreatic ductal adenocarcinoma. European Journal of Nuclear Medicine and Molecular Imaging, 2017, 44, 1995-2003.	6.4	30
72	Comparison of Diagnostic Sensitivity and Quantitative Indices Between 68Ga-DOTATOC PET/CT and 1111n-Pentetreotide SPECT/CT in Neuroendocrine Tumors: a Preliminary Report. Nuclear Medicine and Molecular Imaging, 2015, 49, 284-290.	1.0	29

#	Article	IF	CITATIONS
73	Prostate-Specific Membrane Antigen PET Imaging in Prostate Cancer: Opportunities and Challenges. Korean Journal of Radiology, 2018, 19, 819.	3.4	29
74	Dosimetry of rhenium-188 diethylene triamine penta-acetic acid for endovascular intra-balloon brachytherapy after coronary angioplasty. European Journal of Nuclear Medicine and Molecular Imaging, 2000, 27, 76-82.	2.1	28
75	Superiority of HMPAO Ictal SPECT to ECD Ictal SPECT in Localizing the Epileptogenic Zone. Epilepsia, 2002, 43, 263-269.	5.1	28
76	Heterogeneity Analysis of 18F-FDG Uptake in Differentiating Between Metastatic and Inflammatory Lymph Nodes in Adenocarcinoma of the Lung: Comparison with Other Parameters and its Application in a Clinical Setting. Nuclear Medicine and Molecular Imaging, 2013, 47, 232-241.	1.0	28
77	MRI-Based Attenuation Correction for PET/MRI Using Multiphase Level-Set Method. Journal of Nuclear Medicine, 2016, 57, 587-593.	5.0	28
78	FDG Whole-Body PET/MRI in Oncology: a Systematic Review. Nuclear Medicine and Molecular Imaging, 2017, 51, 22-31.	1.0	28
79	Comparison of the cost-effectiveness of stress myocardial SPECT and stress echocardiography in suspected coronary artery disease considering the prognostic value of false-negative results. Journal of Nuclear Cardiology, 2002, 9, 515-522.	2.1	27
80	Gray matter correlates of dopaminergic degeneration in <scp>P</scp> arkinson's disease: A hybrid <scp>PET/MR</scp> study using ¹⁸ <scp>F</scp> â€ <scp>FP</scp> â€ <scp>CIT</scp> . Human Brain Mapping, 2016, 37, 1710-1721.	3.6	27
81	Diagnostic value of integrated PET/MRI for detection and localization of prostate cancer: Comparative study of multiparametric MRI and PET/CT. Journal of Magnetic Resonance Imaging, 2017, 45, 597-609.	3.4	27
82	Functional evaluation of parathyroid adenoma using 99mTc-MIBI parathyroid SPECT/CT. Nuclear Medicine Communications, 2014, 35, 649-654.	1.1	26
83	Thyroxine-binding globulin, peripheral deiodinase activity, and thyroid autoantibody status in association of phthalates and phenolic compounds with thyroid hormones in adult population. Environment International, 2020, 140, 105783.	10.0	26
84	Lead, mercury, and cadmium exposures are associated with obesity but not with diabetes mellitus: Korean National Environmental Health Survey (KoNEHS) 2015–2017. Environmental Research, 2022, 204, 111888.	7.5	26
85	Gender Differences in Total and Regional Body Composition Changes as Measured by Dual-Energy X-Ray Absorptiometry in Korean Children and Adolescents. Journal of Clinical Densitometry, 2009, 12, 229-237.	1.2	25
86	Reciprocal change in Glucose metabolism of Cancer and Immune Cells mediated by different Glucose Transporters predicts Immunotherapy response. Theranostics, 2020, 10, 9579-9590.	10.0	25
87	Establishment of the Seoul National University Prospectively Enrolled Registry for Genitourinary Cancer (SUPER-GUC): A prospective, multidisciplinary, bio-bank linked cohort and research platform. Investigative and Clinical Urology, 2019, 60, 235.	2.0	25
88	Detection and Characterization of Parathyroid Adenoma/Hyperplasia for Preoperative Localization: Comparison Between 11C-Methionine PET/CT and 99mTc-Sestamibi Scintigraphy. Nuclear Medicine and Molecular Imaging, 2013, 47, 166-172.	1.0	24
89	Segmentation-Based MR Attenuation Correction Including Bones Also Affects Quantitation in Brain Studies: An Initial Result of ¹⁸ F-FP-CIT PET/MR for Patients with Parkinsonism. Journal of Nuclear Medicine, 2014, 55, 1617-1622.	5.0	24
90	Correlation of Asymmetry Indices Measured by Arterial Spin-Labeling MR Imaging and SPECT in Patients with Crossed Cerebellar Diaschisis. American Journal of Neuroradiology, 2015, 36, 1662-1668.	2.4	24

#	Article	IF	CITATIONS
91	Comprehensive gene expression analysis for exploring the association between glucose metabolism and differentiation of thyroid cancer. BMC Cancer, 2019, 19, 1260.	2.6	24
92	Preoperative PET/CT FDG standardized uptake value of pelvic lymph nodes as a significant prognostic factor in patients with uterine cervical cancer. European Journal of Nuclear Medicine and Molecular Imaging, 2014, 41, 674-681.	6.4	23
93	¹⁸ F-FEDAC as a Targeting Agent for Activated Macrophages in DBA/1 Mice with Collagen-Induced Arthritis: Comparison with ¹⁸ F-FDG. Journal of Nuclear Medicine, 2018, 59, 839-845.	5.0	23
94	A diagnostic model to detect silent brain metastases in patients with non-small cell lung cancer. European Journal of Cancer, 2008, 44, 2411-2417.	2.8	22
95	Amyloid PET Quantification Via End-to-End Training of a Deep Learning. Nuclear Medicine and Molecular Imaging, 2019, 53, 340-348.	1.0	22
96	The Value of SPECT/CT in Localizing Pain Site and Prediction of Treatment Response in Patients with Chronic Low Back Pain. Journal of Korean Medical Science, 2014, 29, 1711.	2.5	21
97	Prognostic value of simultaneous 18F-FDG PET/MRI using a combination of metabolo-volumetric parameters and apparent diffusion coefficient in treated head and neck cancer. EJNMMI Research, 2018, 8, 2.	2.5	21
98	Evaluation of Adrenal Masses in Lung Cancer Patients Using F-18 FDG PET/CT. Nuclear Medicine and Molecular Imaging, 2011, 45, 52-58.	1.0	20
99	Prospective Evaluation of Changes in Tumor Size and Tumor Metabolism in Patients with Advanced Gastric Cancer Undergoing Chemotherapy: Association and Clinical Implication. Journal of Nuclear Medicine, 2017, 58, 899-904.	5.0	20
100	Prognostic importance of lymph node-to-primary tumor standardized uptake value ratio in invasive squamous cell carcinoma of uterine cervix. European Journal of Nuclear Medicine and Molecular Imaging, 2017, 44, 1862-1869.	6.4	19
101	Prognostic significance of preoperative ¹⁸ F-FDG PET/CT in uterine leiomyosarcoma. Journal of Gynecologic Oncology, 2017, 28, e28.	2.2	19
102	Preoperative [18F]FDG PET/CT tumour heterogeneity index in patients with uterine leiomyosarcoma: a multicentre retrospective study. European Journal of Nuclear Medicine and Molecular Imaging, 2018, 45, 1309-1316.	6.4	19
103	Abnormal neuroinflammation in fibromyalgia and CRPS using [11C]-(R)-PK11195 PET. PLoS ONE, 2021, 16, e0246152.	2.5	19
104	Reproducibility of assessment of myocardial function using gated 99Tcm-MIBI SPECT and quantitative software. Nuclear Medicine Communications, 2000, 21, 1127-1134.	1.1	18
105	Modulation of Insulin Sensitivity and Caveolin-1 Expression by Orchidectomy in a Nonobese Type 2 Diabetes Animal Model. Molecular Medicine, 2011, 17, 4-11.	4.4	18
106	Prognostic Value of SUVmean in Oropharyngeal and Hypopharyngeal Cancers. Clinical Nuclear Medicine, 2015, 40, 9-13.	1.3	18
107	Composite criteria using clinical and FDG PET/CT factors for predicting recurrence of hepatocellular carcinoma after living donor liver transplantation. European Radiology, 2019, 29, 6009-6017.	4.5	18
108	Diagnostic Accuracy of F-18 FDG-PET in the Assessment of Posttherapeutic Recurrence of Head and Neck Cancer. Molecular Imaging and Biology, 1999, 2, 197-204.	0.3	17

#	Article	IF	CITATIONS
109	Synthesis and Evaluation of <i>cis</i> -1-[4-(Hydroxymethyl)-2-cyclopenten-1-yl]-5-[¹²⁴ 1]iodouracil:  A New Potential PET Imaging Agent for HSV1-tk Expression. Journal of Medicinal Chemistry, 2007, 50, 6032-6038.	6.4	17
110	Effectiveness of [124I]-PET/CT and [18F]-FDG-PET/CT for Localizing Recurrence in Patients with Differentiated Thyroid Carcinoma. Journal of Korean Medical Science, 2012, 27, 1019.	2.5	17
111	Clinical Performance of Whole-Body 18F-FDG PET/Dixon-VIBE, T1-Weighted, and T2-Weighted MRI Protocol in Colorectal Cancer. Clinical Nuclear Medicine, 2015, 40, e392-e398.	1.3	17
112	Measurement of 68Ga-DOTATOC Uptake in the Thoracic Aorta and Its Correlation with Cardiovascular Risk. Nuclear Medicine and Molecular Imaging, 2018, 52, 279-286.	1.0	17
113	Predictive Role of Temporal Changes in Intratumoral Metabolic Heterogeneity During Palliative Chemotherapy in Patients with Advanced Pancreatic Cancer: A Prospective Cohort Study. Journal of Nuclear Medicine, 2020, 61, 33-39.	5.0	17
114	Diagnostic Accuracy and Confidence of [18F] FDG PET/MRI in comparison with PET or MRI alone in Head and Neck Cancer. Scientific Reports, 2020, 10, 9490.	3.3	17
115	Visual interpretation of [18F]Florbetaben PET supported by deep learning–based estimation of amyloid burden. European Journal of Nuclear Medicine and Molecular Imaging, 2021, 48, 1116-1123.	6.4	17
116	Impaired phagocytosis of apoptotic cells causes accumulation of bone marrow-derived macrophages in aged mice. BMB Reports, 2017, 50, 43-48.	2.4	17
117	Relation of EGFR Mutation Status to Metabolic Activity in Localized Lung Adenocarcinoma and Its Influence on the Use of FDG PET/CT Parameters in Prognosis. American Journal of Roentgenology, 2018, 210, 1346-1351.	2.2	16
118	Distinguishing between Thymic Epithelial Tumors and Benign Cysts via Computed Tomography. Korean Journal of Radiology, 2019, 20, 671.	3.4	16
119	Combined radionuclide–chemotherapy and in vivo imaging of hepatocellular carcinoma cells after transfection of a triple-gene construct, NIS, HSV1-sr39tk, and EGFP. Cancer Letters, 2010, 290, 129-138.	7.2	15
120	Feasibility of PET Template-Based Analysis on F-18 FP-CIT PET in Patients with De Novo Parkinson's Disease. Nuclear Medicine and Molecular Imaging, 2013, 47, 73-80.	1.0	15
121	In Vitro Radionuclide Therapy and In Vivo Scintigraphic Imaging of Alpha-Fetoprotein-Producing Hepatocellular Carcinoma by Targeted Sodium Iodide Symporter Gene Expression. Nuclear Medicine and Molecular Imaging, 2013, 47, 1-8.	1.0	15
122	Feasibility of ¹⁸ F-FDG PET as a Noninvasive Diagnostic Tool of Muscle Denervation: A Preliminary Study. Journal of Nuclear Medicine, 2014, 55, 1737-1740.	5.0	15
123	Serum thyroglobulin level after radioiodine therapy (Day 3) to predict successful ablation of thyroid remnant in postoperative thyroid cancer. Annals of Nuclear Medicine, 2015, 29, 184-189.	2.2	15
124	Prognostic value of total lesion glycolysis on preoperative 18F-FDG PET/CT in patients with uterine carcinosarcoma. European Radiology, 2016, 26, 4148-4154.	4.5	15
125	Prognostic value of lymph node-to-primary tumor standardized uptake value ratio in endometrioid endometrial carcinoma. European Journal of Nuclear Medicine and Molecular Imaging, 2018, 45, 47-55.	6.4	15
126	Dopamine dysregulation in psychotic relapse after antipsychotic discontinuation: an [18F]DOPA and [11C]raclopride PET study in first-episode psychosis. Molecular Psychiatry, 2021, 26, 3476-3488.	7.9	15

#	Article	IF	CITATIONS
127	[18F]CB251 PET/MR imaging probe targeting translocator protein (TSPO) independent of its Polymorphism in a Neuroinflammation Model. Theranostics, 2020, 10, 9315-9331.	10.0	15
128	Circulating Osteocalcinâ€Positive Cells as a Novel Diagnostic Biomarker for Bone Metastasis in Breast Cancer Patients. Journal of Bone and Mineral Research, 2020, 35, 1838-1849.	2.8	15
129	Feasibility of Quantitative Flow Ratio–Derived Pullback Pressure Gradient Index and Its Impact on Diagnostic Performance. JACC: Cardiovascular Interventions, 2021, 14, 353-355.	2.9	15
130	Generation of parametric image of regional myocardial blood flow using H(2)(15)O dynamic PET and a linear least-squares method. Journal of Nuclear Medicine, 2005, 46, 1687-95.	5.0	15
131	Imaging of a localized bacterial infection with endogenous thymidine kinase using radioisotope-labeled nucleosides. International Journal of Medical Microbiology, 2012, 302, 101-107.	3.6	14
132	The Effectiveness of Recombinant Human Thyroid-Stimulating Hormone versus Thyroid Hormone Withdrawal Prior to Radioiodine Remnant Ablation in Thyroid Cancer: A Meta-Analysis of Randomized Controlled Trials. Journal of Korean Medical Science, 2014, 29, 811.	2.5	14
133	Correlation of 11C-methionine PET and diffusion-weighted MRI. Nuclear Medicine Communications, 2014, 35, 720-726.	1.1	14
134	Pixelized Measurement of 99mTc-HDP Micro Particles Formed in Gamma Correction Phantom Pinhole Scan: a Reference Study. Nuclear Medicine and Molecular Imaging, 2016, 50, 207-212.	1.0	14
135	Efficacy and Safety of Human Serum Albumin–Cisplatin Complex in U87MG Xenograft Mouse Models. International Journal of Molecular Sciences, 2020, 21, 7932.	4.1	14
136	3′-Deoxy-3′-[18F]fluorothymidine and O-(2-[18F]fluoroethyl)-L-tyrosine PET in Patients with Suspicious Recurrence of Glioma after Multimodal Treatment: Initial Results of a Retrospective Comparative Study. Nuclear Medicine and Molecular Imaging, 2010, 44, 45-54.	1.0	13
137	Preoperative PET/CT standardized FDG uptake values of pelvic lymph nodes as a significant prognostic factor in patients with endometrial cancer. European Journal of Nuclear Medicine and Molecular Imaging, 2014, 41, 1793-1799.	6.4	13
138	Prediction of Recurrence by Preoperative Intratumoral FDG Uptake Heterogeneity in Endometrioid Endometrial Cancer. Translational Oncology, 2017, 10, 178-183.	3.7	13
139	Prediction of breast cancer recurrence using lymph node metabolic and volumetric parameters from 18F-FDG PET/CT in operable triple-negative breast cancer. European Journal of Nuclear Medicine and Molecular Imaging, 2017, 44, 1787-1795.	6.4	13
140	Development of 99mTc-Labeled Human Serum Albumin with Prolonged Circulation by Chelate-then-Click Approach: A Potential Blood Pool Imaging Agent. Molecular Pharmaceutics, 2019, 16, 1586-1595.	4.6	13
141	Identification of alternative protein targets of glutamate-ureido-lysine associated with PSMA tracer uptake in prostate cancer cells. Proceedings of the National Academy of Sciences of the United States of America, 2022, 119, .	7.1	13
142	Syntheses of F-18 labeled fluoroalkyltyrosine derivatives and their biological evaluation in rat bearing 9L tumor. Bioorganic and Medicinal Chemistry Letters, 2007, 17, 200-204.	2.2	12
143	Clinical significance of 18F-FDG uptake by primary sites in patients with diffuse large B cell lymphoma in the head and neck: a pilot study. Annals of Nuclear Medicine, 2008, 22, 645-651.	2.2	12
144	Clinical significance of 18F-FDG uptake by N2 lymph nodes in patients with resected stage IIIA N2 non-small-cell lung cancer: A retrospective study. Lung Cancer, 2008, 60, 69-74.	2.0	12

#	Article	IF	CITATIONS
145	Application of bioluminescence imaging to therapeutic intervention of herpes simplex virus type I – Thymidine kinase/ganciclovir in glioma. Cancer Letters, 2010, 297, 84-90.	7.2	12
146	<i>In vivo</i> bioluminescent imaging of αâ€fetoproteinâ€producing hepatocellular carcinoma in the diethylnitrosamineâ€treated mouse using recombinant adenoviral vector. Journal of Gene Medicine, 2012, 14, 513-520.	2.8	12
147	Dual-time point 18F-FDG PET/CT for the staging of oesophageal cancer: the best diagnostic performance by retention index for N-staging in non-calcified lymph nodes. European Journal of Nuclear Medicine and Molecular Imaging, 2018, 45, 1317-1328.	6.4	12
148	InÂvivo imaging of activated macrophages by 18F-FEDAC, a TSPO targeting PET ligand, in the use of biologic disease-modifying anti-rheumatic drugs (bDMARDs). Biochemical and Biophysical Research Communications, 2018, 506, 216-222.	2.1	12
149	Application of Quantitative Indexes of FDG PET to Treatment Response Evaluation in Indolent Lymphoma. Nuclear Medicine and Molecular Imaging, 2018, 52, 342-349.	1.0	12
150	Clinicopathologic risk factors of radioactive iodine therapy based on response assessment in patients with differentiated thyroid cancer: a multicenter retrospective cohort study. European Journal of Nuclear Medicine and Molecular Imaging, 2020, 47, 561-571.	6.4	12
151	Association of Quantitative Flow Ratio with Lesion Severity and Its Ability to Discriminate Myocardial Ischemia. Korean Circulation Journal, 2021, 51, 126.	1.9	12
152	Development of a method for measuring myocardial contractility with gated myocardial SPECT and arterial tonometry. Journal of Nuclear Cardiology, 1999, 6, 657-671.	2.1	11
153	Synthesis and evaluation of aryl-substituted diarylpropionitriles, selective ligands for estrogen receptor β, as positron-emission tomographic imaging agents. Bioorganic and Medicinal Chemistry, 2009, 17, 3479-3488.	3.0	11
154	Non-invasive monitoring of hepatocellular carcinoma in transgenic mouse with bioluminescent imaging. Cancer Letters, 2011, 310, 53-60.	7.2	11
155	18F-Fluorodeoxyglucose and 11C-methionine positron emission tomography in relation to methyl-guanine methyltransferase promoter methylation in high-grade gliomas. Nuclear Medicine Communications, 2015, 36, 211-218.	1.1	11
156	Fluorine-18 fluorodeoxyglucose positron emission tomography imaging of T-lymphoblastic lymphoma patients. Oncology Letters, 2016, 12, 1620-1622.	1.8	11
157	Clinical Significance of Pretreatment FDG PET/CT in MIBG-Avid Pediatric Neuroblastoma. Nuclear Medicine and Molecular Imaging, 2017, 51, 154-160.	1.0	11
158	Comparison of Quantitative Methods on FDG PET/CT for Treatment Response Evaluation of Metastatic Colorectal Cancer. Nuclear Medicine and Molecular Imaging, 2017, 51, 147-153.	1.0	11
159	Therapeutic efficacy of modified anti-miR21 in metastatic prostate cancer. Biochemical and Biophysical Research Communications, 2020, 529, 707-713.	2.1	11
160	A pan-cancer analysis of the clinical and genetic portraits of somatostatin receptor expressing tumor as a potential target of peptide receptor imaging and therapy. EJNMMI Research, 2020, 10, 42.	2.5	11
161	Criteria for definition of regional functional improvement on quantitative post-stress gated myocardial SPET after bypass surgery in patients with ischaemic cardiomyopathy. European Journal of Nuclear Medicine and Molecular Imaging, 2002, 29, 1078-1082.	6.4	10
162	Cellular metabolic responses of PET radiotracers to 188Re radiation in an MCF7 cell line containing dominant-negative mutant p53. Nuclear Medicine and Biology, 2007, 34, 425-432.	0.6	10

#	Article	IF	CITATIONS
163	Feasibility of Template-Guided Attenuation Correction in Cat Brain PET Imaging. Molecular Imaging and Biology, 2010, 12, 250-258.	2.6	10
164	Total lesion glycolysis as the best 18F-FDG PET/CT parameter in differentiating intermediate–high risk adrenal incidentaloma. Nuclear Medicine Communications, 2014, 35, 606-612.	1.1	10
165	Association between partial-volume corrected SUVmax and Oncotype DX recurrence score in early-stage, ER-positive/HER2-negative invasive breast cancer. European Journal of Nuclear Medicine and Molecular Imaging, 2016, 43, 1574-1584.	6.4	10
166	Prognostic Value of 68Ga-NOTA-RGD PET/CT for Predicting Disease-Free Survival for Patients With Breast Cancer Undergoing Neoadjuvant Chemotherapy and Surgery. Clinical Nuclear Medicine, 2016, 41, 614-620.	1.3	10
167	Appropriate margin thresholds for isocontour metabolic volumetry of fluorine-18 fluorodeoxyglucose PET in sarcoma. Nuclear Medicine Communications, 2016, 37, 1088-1094.	1.1	10
168	Comparison of Two Different Segmentation Methods on Planar Lung Perfusion Scan with Reference to Quantitative Value on SPECT/CT. Nuclear Medicine and Molecular Imaging, 2017, 51, 161-168.	1.0	10
169	Correlation of FDG PET/CT Findings with Long-Term Growth and Clinical Course of Abdominal Aortic Aneurysm. Nuclear Medicine and Molecular Imaging, 2018, 52, 46-52.	1.0	10
170	Intracavitary Radiation Therapy for Recurrent Cystic Brain Tumors with Holmium-166-Chico : A Pilot Study. Journal of Korean Neurosurgical Society, 2013, 54, 175.	1.2	10
171	Parametric image of myocardial blood flow generated from dynamic H2 15O PET using factor analysis and cluster analysis. Medical and Biological Engineering and Computing, 2005, 43, 678-685.	2.8	9
172	Squamous Cell Carcinoma Arising From Pulmonary Hamartoma. Clinical Nuclear Medicine, 2011, 36, 130-131.	1.3	9
173	Increased 18F-FDG uptake in the trapezius muscle in patients with spinal accessory neuropathy. Journal of the Neurological Sciences, 2016, 362, 127-130.	0.6	9
174	Recurrence of Melanoma After Initial Treatment: Diagnostic Performance of FDG PET in Posttreatment Surveillance. Nuclear Medicine and Molecular Imaging, 2018, 52, 327-333.	1.0	9
175	Development of 99mTc-labeled trivalent isonitrile radiotracer for folate receptor imaging. Bioorganic and Medicinal Chemistry, 2019, 27, 1925-1931.	3.0	9
176	Relationship of EGFR Mutation to Glucose Metabolic Activity and Asphericity of Metabolic Tumor Volume in Lung Adenocarcinoma. Nuclear Medicine and Molecular Imaging, 2020, 54, 175-182.	1.0	9
177	Unsupervised clustering of dopamine transporter <scp>PET</scp> imaging discovers heterogeneity of parkinsonism. Human Brain Mapping, 2020, 41, 4744-4752.	3.6	9
178	Risk stratification of symptomatic brain metastases by clinical and FDG PET parameters for selective use of prophylactic cranial irradiation in patients with extensive disease of small cell lung cancer. Radiotherapy and Oncology, 2020, 143, 81-87.	0.6	9
179	Head to head comparison of 68Ga-NGUL and 68Ga-PSMA-11 in patients with metastatic prostate cancer: a prospective study. Journal of Nuclear Medicine, 2021, 62, jnumed.120.258434.	5.0	9
180	Consideration of perfusion reserve in viability assessment by myocardial Tl-201 rest-redistribution SPECT: A quantitative study with dual-isotope SPECT. Journal of Nuclear Cardiology, 2002, 9, 68-74.	2.1	8

#	Article	IF	CITATIONS
181	Prodrug-activating Gene Therapy with Rabbit Cytochrome P450 4B1/4-Ipomeanol or 2-Aminoanthracene System in Glioma Cells. Nuclear Medicine and Molecular Imaging, 2010, 44, 193-198.	1.0	8
182	PET/MR Imaging for Chest Diseases. Magnetic Resonance Imaging Clinics of North America, 2015, 23, 245-259.	1.1	8
183	Usefulness of Additional SPECT/CT Identifying Lymphatico-renal Shunt in a Patient with Chyluria. Nuclear Medicine and Molecular Imaging, 2015, 49, 61-64.	1.0	8
184	Intramyocardial Adipose-Derived Stem Cell Transplantation Increases Pericardial Fat with Recovery of Myocardial Function after Acute Myocardial Infarction. PLoS ONE, 2016, 11, e0158067.	2.5	8
185	Prognostic implication of the metastatic lesion-to-ovarian cancer standardised uptake value ratio in advanced serous epithelial ovarian cancer. European Radiology, 2017, 27, 4510-4515.	4.5	8
186	Adenine Nucleotide Translocase 2 as an Enzyme Related to [18F] FDG Accumulation in Various Cancers. Molecular Imaging and Biology, 2019, 21, 722-730.	2.6	8
187	A comparative study of 188Re(V)-meso-DMSA and 188Re(V)-rac-DMSA: preparation and in vivo evaluation in nude mice xenografted with a neuroendocrine tumor. Nuclear Medicine and Biology, 2007, 34, 1029-1036.	0.6	7
188	<i>Short Commmunication:</i> Synthesis and Biologic Evaluation of I-123-Labeled Porphyrin Derivative as a Potential Tumor-Imaging Agent. Cancer Biotherapy and Radiopharmaceuticals, 2007, 22, 853-862.	1.0	7
189	Radioiodination and biodistribution of quantum dots using Bolton–Hunter reagent. Applied Radiation and Isotopes, 2011, 69, 56-62.	1.5	7
190	A Hepatoid Adenocarcinoma of the Stomach Evaluated With 18F-FDG PET/CT. Clinical Nuclear Medicine, 2014, 39, 442-445.	1.3	7
191	Phase analysis of gated myocardial perfusion single-photon emission computed tomography after coronary artery bypass graft surgery. Nuclear Medicine Communications, 2016, 37, 1139-1147.	1.1	7
192	Feasibility of simultaneous 18F-FDG PET/MRI for the quantitative volumetric and metabolic measurements of abdominal fat tissues using fat segmentation. Nuclear Medicine Communications, 2016, 37, 616-622.	1.1	7
193	Prospective Evaluation of the Clinical Implications of the Tumor Metabolism and Chemotherapy-Related Changes in Advanced Biliary Tract Cancer. Journal of Nuclear Medicine, 2017, 58, 1255-1261.	5.0	7
194	The New Possibility of Lymphoscintigraphy to Guide a Clinical Treatment for Lymphedema in Patient With Breast Cancer. Clinical Nuclear Medicine, 2019, 44, 179-185.	1.3	7
195	Synthesis and Evaluation of 99mTc-Tricabonyl Labeled Isonitrile Conjugates for Prostate-Specific Membrane Antigen (PSMA) Image. Inorganics, 2020, 8, 5.	2.7	7
196	Effects of structural differences between radioiodine-labeled 1-(2′-fluoro-2′-deoxy-d-arabinofuranosyl)-5-iodouracil (FIAU) and 1-(2′-fluoro-2′-deoxy-d-ribofuranosyl)-5-iodouracil (FIRU) on HSV1-TK reporter gene imaging. Applied Radiation and Isotopes, 2010, 68, 971-978.	1.5	6
197	Monitoring differentiated thyroid cancer patients with negative serum thyroglobulin. Nuklearmedizin - NuclearMedicine, 2014, 53, 32-38.	0.7	6
198	Bilateral Renal Metastasis of Hürthle Cell Thyroid Cancer with Discordant Uptake Between I-131 Sodium Iodide and F-18 FDG. Nuclear Medicine and Molecular Imaging, 2017, 51, 256-260.	1.0	6

#	Article	IF	CITATIONS
199	Spleen Scan for 68Ga-DOTATOC PET-Positive Pancreatic Tail Lesion: Differential Diagnosis of Neuroendocrine Tumor from Accessory Spleen. Nuclear Medicine and Molecular Imaging, 2020, 54, 43-47.	1.0	6
200	Variability of FP-CIT PET Patterns Associated With Clinical Features of Multiple System Atrophy. Neurology, 2021, 96, e1663-e1671.	1.1	6
201	Prospective evaluation of metabolic intratumoral heterogeneity in patients with advanced gastric cancer receiving palliative chemotherapy. Scientific Reports, 2021, 11, 296.	3.3	6
202	Registration Method for the Detection of Tumors in Lung and Liver Using Multimodal Small Animal Imaging. IEEE Transactions on Nuclear Science, 2009, 56, 1454-1458.	2.0	5
203	The Prevalence and Characteristics of Brown Adipose Tissue in an 18F-FDG PET Study of Koreans. Nuclear Medicine and Molecular Imaging, 2010, 44, 207-212.	1.0	5
204	Parametric Cerebrovascular Reserve Images Using Acetazolamide 99mTc-HMPAO SPECT: A Feasibility Study of Quantitative Assessment. Nuclear Medicine and Molecular Imaging, 2013, 47, 188-195.	1.0	5
205	Incidental thyroid cancer detected by 18F-FDG PET. Nuclear Medicine Communications, 2014, 35, 453-458.	1.1	5
206	Hemodynamic Significance of Internal Carotid or Middle Cerebral Artery Stenosis Detected on Magnetic Resonance Angiography. Yonsei Medical Journal, 2015, 56, 1686.	2.2	5
207	Plasmablastic lymphoma exclusively involving bones mimicking osteosarcoma in an immunocompetent patient. Medicine (United States), 2016, 95, e4241.	1.0	5
208	Prognostic importance of peritoneal lesion-to-primary tumour standardized uptake value ratio in advanced serous epithelial ovarian cancer. European Radiology, 2018, 28, 2107-2114.	4.5	5
209	18F-FDG positron emission tomography as a novel diagnostic tool for peripheral nerve injury. Journal of Neuroscience Methods, 2019, 317, 11-19.	2.5	5
210	Glucose-6-phosphatase Expression–Mediated [18F]FDG Efflux in Murine Inflammation and Cancer Models. Molecular Imaging and Biology, 2019, 21, 917-925.	2.6	5
211	Comparison of Cellular Metabolic Responses of 18F-FDG According to the Effect of ² -Irradiation in p53 Wild and Deleted Cell Lines. Cancer Biotherapy and Radiopharmaceuticals, 2007, 22, 636-643.	1.0	4
212	Synthesis of novel phytosphingosine derivatives and their preliminary biological evaluation for enhancing radiation therapy. Bioorganic and Medicinal Chemistry Letters, 2007, 17, 6643-6646.	2.2	4
213	F-18 FDG PET-CT Imaging of Intestinal Metastasis From Primary Lung Cancer. Clinical Nuclear Medicine, 2008, 33, 870-871.	1.3	4
214	Significance of smoking history and FDG uptake for pathological N2 staging in clinical N2-negative non-small-cell lung cancer. Annals of Oncology, 2011, 22, 2068-2072.	1.2	4
215	Peripheral Bone Involvement of Intravascular Large B-Cell Lymphoma on 99mTc-MDP Bone Scan and 18F-FDG PET/CT. Clinical Nuclear Medicine, 2012, 37, 810-811.	1.3	4
216	Non-Ischemic Perfusion Defects due to Delayed Arrival of Contrast Material on Stress Perfusion Cardiac Magnetic Resonance Imaging after Coronary Artery Bypass Graft Surgery. Korean Journal of Radiology, 2014, 15, 188.	3.4	4

#	Article	IF	CITATIONS
217	Sodium Iodide Symporter (NIS) in the Management of Patients with Thyroid Carcinoma. Nuclear Medicine and Molecular Imaging, 2018, 52, 325-326.	1.0	4
218	Nuclear Theranostics in Asia: In vivo Companion Diagnostics. Nuclear Medicine and Molecular Imaging, 2019, 53, 1-6.	1.0	4
219	Spatial Normalization Using Early-Phase [18F]FP-CIT PET for Quantification of Striatal Dopamine Transporter Binding. Nuclear Medicine and Molecular Imaging, 2020, 54, 305-314.	1.0	4
220	Synthesis and Evaluation of F-18 Labeled 2'-Deoxy-2'-fluoro-5-methyl-1-β-L-arabinofuranosyluracil (L-[18F]FMAU). Bulletin of the Korean Chemical Society, 2007, 28, 2449-2453.	1.9	4
221	Synthesis and Evaluation of Estrogen Receptor β -Selective Ligands: Fluoroalkylated Indazole Estrogens. Bulletin of the Korean Chemical Society, 2008, 29, 1107-1114.	1.9	4
222	Exposure to Bisphenol A, S, and F and its Association with Obesity and Diabetes Mellitus in General Adults of Korea: Korean National Environmental Health Survey (KoNEHS) 2015–2017. Exposure and Health, 2023, 15, 53-67.	4.9	4
223	Detectability of T-Measurable Diseases in Advanced Gastric Cancer on FDG PET-CT. Nuclear Medicine and Molecular Imaging, 2012, 46, 261-268.	1.0	3
224	Evaluation of Azygous Vein Aneurysm Using Integrated PET/MRI. Nuclear Medicine and Molecular Imaging, 2014, 48, 161-162.	1.0	3
225	Malignant Peritoneal Mesothelioma Masquerades as Peritoneal Metastasis on 18F-FDG PET/CT Scans; a Rare Diagnosis that Should Not Be Missed. Nuclear Medicine and Molecular Imaging, 2015, 49, 325-328.	1.0	3
226	Identification of Metabolic Biomarkers Using Serial 18 F–FDG PET/CT for Prediction of Recurrence in Advanced Epithelial Ovarian Cancer. Translational Oncology, 2017, 10, 297-303.	3.7	3
227	¹⁸ Fâ€FDG uptake in denervated muscles of patients with peripheral nerve injury. Annals of Clinical and Translational Neurology, 2019, 6, 2175-2185.	3.7	3
228	Clinical implication of 18F-NaF PET/computed tomography indexes of aortic calcification in coronary artery disease patients: correlations with cardiovascular risk factors. Nuclear Medicine Communications, 2020, 41, 58-64.	1.1	3
229	The Potential Roles of Radionanomedicine and Radioexosomics in Prostate Cancer Research and Treatment. Current Pharmaceutical Design, 2017, 23, 2976-2990.	1.9	3
230	Presurgical Mapping of Brain Tumors Using Statistical Probabilistic Anatomical Maps. Journal of Biomedical Science and Engineering, 2015, 08, 653-658.	0.4	3
231	A Negative Correlation Between Blood Glucose Level and 68ÂGa-DOTA-TOC Uptake in the Pancreas Uncinate Process. Nuclear Medicine and Molecular Imaging, 2022, 56, 52-58.	1.0	3
232	Sex, menopause, and age differences in the associations of persistent organic pollutants with thyroid hormones, thyroxine-binding globulin, and peripheral deiodinase activity: A cross-sectional study of the general Korean adult population. Environmental Research, 2022, 212, 113143.	7.5	3
233	A Case of Severe Protein-losing Enteropathy as a Late Complication of Pelvic Irradiation. Korean Journal of Internal Medicine, 2004, 19, 271-275.	1.7	2
234	Clinical Role of F-18 Fluorodeoxyglucose Positron Emission Tomography for Follow-up of Patients with Renal Cell Carcinoma. Korean Journal of Urology, 2007, 48, 765.	0.2	2

#	Article	IF	CITATIONS
235	Phase II study of evofosfamide (TH-302) monotherapy as a second-line treatment in advanced biliary tract cancer. Annals of Oncology, 2018, 29, viii259.	1.2	2
236	Effects of Maternal lodine Status during Pregnancy and Lactation on Maternal Thyroid Function and Offspring Growth and Development: A Prospective Study Protocol for the Ideal Breast Milk Cohort. Endocrinology and Metabolism, 2018, 33, 395.	3.0	2
237	Diagnostic Performance of Nonhyperemic Pressure Ratios Assessed by 13N-Ammonium Positron Emission Tomography. JACC: Cardiovascular Interventions, 2019, 12, 1517-1518.	2.9	2
238	Predicting outcome of repair of medial meniscus posterior root tear with early osteoarthritis using bone single-photon emission computed tomography/computed tomography. Medicine (United States), 2020, 99, e21047.	1.0	2
239	Rosai-Dorfman Disease: Importance of 18F FDG PET/CT to Determine Extension and Extranodal Involvement. Nuclear Medicine and Molecular Imaging, 2021, 55, 146-148.	1.0	2
240	Targeting Hypoxia Using Evofosfamide and Companion Hypoxia Imaging of FMISO-PET in Advanced Biliary Tract Cancer. Cancer Research and Treatment, 2021, 53, 471-479.	3.0	2
241	Limited implication of initial bone scintigraphy on longâ€ŧerm condylar bone change in temporomandibular disorders—Comparison with cone beam computed tomography at 1Âyear. Journal of Oral Rehabilitation, 2021, 48, 880-890.	3.0	2
242	Glucose metabolic profiles evaluated by PET associated with molecular characteristic landscape of gastric cancer. Gastric Cancer, 2021, , 1.	5.3	2
243	Effect of TSH stimulation protocols on adequacy of low-iodine diet for radioiodine administration. PLoS ONE, 2021, 16, e0256727.	2.5	2
244	FDG-PET in Mediastinal Nodal Staging of Non-small Cell Lung Cancer: Correlation of False Results with Histopathologic Finding. Cancer Research and Treatment, 2003, 35, 232-238.	3.0	2
245	Role of PET Scan in Gastric Cancer as a Diagnostic Tool. Journal of Gastric Cancer, 2002, 2, 184.	2.5	2
246	Relationship Between Ktrans and K1 with Simultaneous Versus Separate MR/PET in Rabbits with VX2 Tumors. Anticancer Research, 2017, 37, 1139-1148.	1.1	2
247	Phase 1 Study of No-Carrier Added 177Lu-DOTATATE (SNU-KB-01) in Patients with Somatostatin Receptor–Positive Neuroendocrine Tumors: The First Clinical Trial of Peptide Receptor Radionuclide Therapy in Korea. Cancer Research and Treatment, 2023, 55, 334-343.	3.0	2
248	Phase I Clinical Trial of Prostate-Specific Membrane Antigen-Targeting ⁶⁸ Ga-NGUL PET/CT in Healthy Volunteers and Patients with Prostate Cancer. Korean Journal of Radiology, 0, 23, .	3.4	2
249	Optimal PET acquisition setting of 1-124 with Siemens Inveon PET: Comparative simulation study with F-I 8 and microPET R4. , 2009, , .		1
250	Is it Feasible to Use the Commercially Available Autoquantitation Software for the Evaluation of Myocardial Viability on Small-Animal Cardiac F-18 FDG PET Scan?. Nuclear Medicine and Molecular Imaging, 2013, 47, 104-114.	1.0	1
251	Comparative characteristics of quantitative indexes for 18F-FDG uptake and metabolic volume in sequentially obtained PET/MRI and PET/CT. Nuclear Medicine Communications, 2017, 38, 333-339.	1.1	1
252	Comparison of D-[18. Bulletin of the Korean Chemical Society, 2010, 31, 3309-3312.	1.9	1

#	Article	IF	CITATIONS
253	New Trends in Radioiodine Treatment for the Advanced Differentiated Thyroid Cancer. The Korean Journal of Endocrine Surgery, 2011, 11, 139.	0.1	1
254	Prospective evaluation of the clinical implications of the tumor metabolism and chemotherapy-related changes in advanced biliary tract cancer Journal of Clinical Oncology, 2017, 35, 261-261.	1.6	1
255	Conjugation of arginylglycylaspartic acid to human serum albumin decreases the tumor-targeting effect of albumin by hindering its secreted protein acidic and rich in cysteine-mediated accumulation in tumors. American Journal of Translational Research (discontinued), 2020, 12, 2488-2498.	0.0	1
256	Respiratory Gating of MicroPET and Clinical CT Studies Using List-mode Acquisition. , 2006, , .		0
257	Gallbladder Cancer Presenting as an Isolated Large Lung Mass. Clinical Nuclear Medicine, 2009, 34, 827-828.	1.3	0
258	Clinical Characteristics of 16 Patients with Pituitary Tumor Incidentally Detected by18F-Fluorodeoxyglucose PET-CT (18F-FDG PET-CT). Endocrinology and Metabolism, 2010, 25, 321.	3.0	0
259	Development of assessment technology for a rat myocardial infarct model using integrated PET/CT and MRI images. , 2010, , .		0
260	FDG-PET/CT Complements Bone Scan with Respect to the Detection of Skip Metastasis of Osteosarcoma: A Case Report. The Journal of the Korean Bone and Joint Tumor Society, 2012, 18, 45.	0.0	0
261	High Serum Levels of Thyroid-Stimulating Hormone and Sustained Weight Gain in Patients with Thyroid Cancer Undergoing Radioiodine Therapy. International Journal of Thyroidology, 2016, 9, 19.	0.1	0
262	Determination of real-time tumor oxygenation changes following high-dose radiotherapy in orthotopic and subcutaneous lung cancers in mice. Journal of Thoracic Oncology, 2016, 11, S27.	1.1	0
263	Sex difference in cardiac metabolism in nonischemic heart failure: Insight for prognostic value of altered cardiac metabolism. Journal of Nuclear Cardiology, 2017, 24, 1236-1238.	2.1	0
264	Discrepancy Between Tumor Antigen Distribution and Radiolabeled Antibody Binding in a Nude Mouse Xenograft Model of Human Melanoma. Cancer Biotherapy and Radiopharmaceuticals, 2017, 32, 83-89.	1.0	0
265	Prostatic Tumors. , 2017, , 95-167.		0
266	Potential clinical utility of a novel optical tomographic imaging for the quantitative assessment of hand rheumatoid arthritis. Rheumatology International, 2019, 39, 2103-2110.	3.0	0
267	Efficacy of voxel-based dosimetry map for predicting response to trans-arterial radioembolization therapy for hepatocellular carcinoma. Nuclear Medicine Communications, 2021, Publish Ahead of Print, 1396-1403.	1.1	0
268	P1-056: The clinical significance of solitary extrathoracic abnormality on whole body FDG-PET in patients with NSCLC. Journal of Thoracic Oncology, 2007, 2, S572.	1.1	0
269	Preparation of 125. Bulletin of the Korean Chemical Society, 2010, 31, 2649-2655.	1.9	Ο
270	Association of reduction of tumor metabolism with prognosis of advanced gastric cancer patients treated with palliative chemotherapy: Prospective cohort study Journal of Clinical Oncology, 2016, 34, 31-31.	1.6	0

#	Article	IF	CITATIONS
271	Predictive role of temporal changes in intratumoral metabolic heterogeneity during palliative chemotherapy in advanced pancreatic cancer patients: A prospective cohort study Journal of Clinical Oncology, 2019, 37, 311-311.	1.6	0
272	Prospective evaluation of metabolic intratumoral heterogeneity using 18F-FDG-PET-CT in patients with advanced gastric cancer receiving palliative chemotherapy Journal of Clinical Oncology, 2019, 37, 4059-4059.	1.6	0
273	Visualization of a novel human monoclonal antibody against Claudin-3 for targeting ovarian cancer. Nuclear Medicine and Biology, 2022, 114-115, 135-142.	0.6	0